

IN-DEPTH DETECTION AND RECONSTRUCTION TECHNIQUES USING HIGH-FREQUENCY MICROWAVES FOR NON-DESTRUCTIVE TESTING ON MULTI-LAYERED COMPOSITE MATERIALS

A. Brook^{*1}, E. Cristofani¹, M. Vandewal¹, C. Matheis² and J. Jonuscheit²

¹Royal Military Academy, CISS Department
Renaissancelaan 30, B-1000 Brussels, Belgium Tel: +32 2 742 6661, Fax: +32 2 742 6472,
Email: anna.brook@elec.rma.ac.be, edison.cristofani@elec.rma.ac.be, marijke.vandewal@rma.ac.be

²Fraunhofer Institute for Physical Measurements Techniques
Erwin-Schrodinger 46, Kaiserslautern, Germany Tel: +49 631 205 5107, Fax: +49 631 205 3902
Email: joachim.jonuscheit@ipm.fraunhofer.de

ABSTRACT

The quality control of aeronautics composite multi-layered materials and structures using non-destructive testing is the main focus of this work. The study proposes a semi-automatic and near real-time mode-operated image processing methodology developed for frequency-modulated continuous-wave high-frequency millimeter wave imagery with the center frequencies around: 100 GHz, 150 GHz and 300 GHz. Image processing is applied on the 3-D images to detect internal defects within the material, which are almost transparent at these frequencies.

Keywords: Target Reconstruction and Detection, Image Processing, NDT, FMCW mmW imagery

1. Introduction

In various practical imagery-based applications, the classification techniques are appropriate to the different types of target detection and each one matches particular target attributes (e.g. spatial and frequency characteristics). The main condition for the imagery data is to provide a suitable quality, which is compatible with the detection algorithms and reference prototype information. The principle of classification is setting pixels of the target to a spatial group data item (class membership) within the image. This relationship is not a function, but has to be described more generally by a probability distribution assuming that the data contains independent samples. In unsupervised classification any individual pixel is compared to each discrete cluster, where the classifier decides which cluster is closest. In a supervised classification the interpreter knows targets are present in the image. All pixels in the image are compared with the class discriminates derived from the training sets. The result is a map of established classes which can be reasonably accurate, but some pixels might be misclassified.

Data classification is performed by two main approaches: the first one considers only a dichotomous distinction between the two classes (K-Means [1]); the second one attempts to model the probability of class membership (Maximum Likelihood [2] and Bayesian classifier [3]). In practice, most of the practical applications are known to be dichotomous supervised, as they require a representative database to support the reliable target detection. However, this approach would not be applicable to the detection of unknown or poorly determined targets. In case of partially available information (e.g. dimensions and general characteristics) a three-dimensional (3-D) mathematical model of the target can be generated and undergo the semi-supervised approach. Else, the data should be introduced to the unsupervised techniques.

Nowadays there has been a significant interest in employing high-frequency millimeter wave (mmW) imagery for many industrial oriented and security applications [4-6]. Among a list of possible applications, quality control of aeronautics composite multi-layered materials and structures through Non-Destructive Testing (NDT) was proposed [7-8]. In the domain of microwave NDT systems [9-13], mmW waves could be used detect visualize and evaluate hidden internal defects within the composite material under test by exploiting 3-D imaging and the transparency property of most non-metal objects in the sub-THz range. One exception is the visualization of carbon fiber composites for which only surface and subsurface defects could be recognized.

The present study proposes semi-supervised and near real-time mode-operated image processing methodology developed for Frequency-Modulated Continuous-Wave (FMCW) mmW images with center frequencies around 100 GHz, 150 GHz and 300 GHz. The quality control of aeronautics composite multi-layered materials and structures (e.g. laminates, fiberglass, Rohacell etc.) using NDT is the main focus of this work. The proposed chain of image processing consists of following data investigation: pre-processing to calculate descriptive statistics, application of a multi-phase process to detect internal targets and post-processing to evaluate the overall accuracy of detection. The methodology is applied on real data, containing manufactured calibration materials, which are commonly used in aeronautics and aerospace industries. The rest of this paper is organized as follows: Section 2 presents the methodology by introducing the concept of image process and target detection. Results are reported in Section 3. Discussions and conclusions are included in the final section.

2. Methodology

The hierarchically structured image processing methodology is exclusively developed to extract and classify the internal (in-depth) defects within the 3-D composite materials. This method is executed on the 3-D FMCW imagery obtained for the manufactured calibration object¹ by validated focus imagery system in terms of precision, accuracy, sensitivity, specificity, uncertainty and robustness. The general terminology is presented in Figure 1 and distinguishes between foreground (related to the object under investigation) and background parts of the image and presents three potential faces (views) for detailed process and analysis: front-, top- and profile- views.

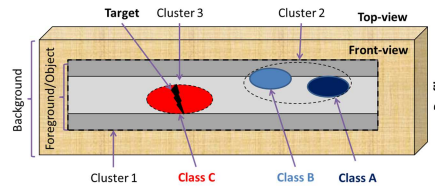


Figure 1. Visualization of the terminology using a generic environment. The 3-D imagery provides three possible views: front, top and profile. Global-level segmentation produces general imagery background and foreground corresponding to the multi-layered (grayscale) object under investigation. Local-level classification provides clusters (dashed areas) and classes (colored areas).

The suggested image processing methodology is not limited by the scanning acquisition system in terms of setup (optics components), scanning mode (reflection/transmission) or operational frequency (100 GHz, 150 GHz or 300 GHz) and it allows both 2-D and 3-D processing. The complete method (Figure 2) is a semi-supervised process, which allows subjective intervention in three stages: (i) selection of a suitable processing method, (ii) training of classifiers by providing manually selected sets of area of interest and (iii) choice of suitable sets for data integration and fusion which leads to accurate identification of the targets and tested by the post-processing stage. The system operator is requested to identify the nature of the object (type of material and overall shape) under investigation at the beginning of the image processing chain, and the nature of the targets (potential defects a priori categorized based on patterns and shapes) just before the analysis stage.

The pre-processing step is a univariate data analysis using basic and descriptive (Figure 2). The calculation of mean, standard deviation, variance, skewness, t-test and F-test contributes additional information to the image pre-processing. The investigation of outliers is prompted by large skewness scores and it is evaluated as an uncertainty level of the image. The first phase of image processing performs segmentation (the split-and-merge technique [14]) computed as an independent constructive solution to the global and nonintersecting noisy background and foreground regions of the image. The second phase of image processing consists of estimating the Area Of Interest (AOI) associated with the different clusters. The multilevel segmentation is adopting a series of consecutively applied unsupervised and semi-supervised learning classification methods [15-16]. The processed top- and profile-(in-depth) view images are gathered into 3-D volume imagery. The reconstructed Volume Of Interest (VOI) containing the results of the AOI detection stage in general and the results of segmentation/classification process in particular. The 3-D location of each class is extracted from the volume imagery and forward-projected on the 2-D front-view image using the internal geometry and dimensions of the scanned object. Finally, the multi-source (different setups, scanning modes and operational frequencies) data are registered by the feature-based registration technique.

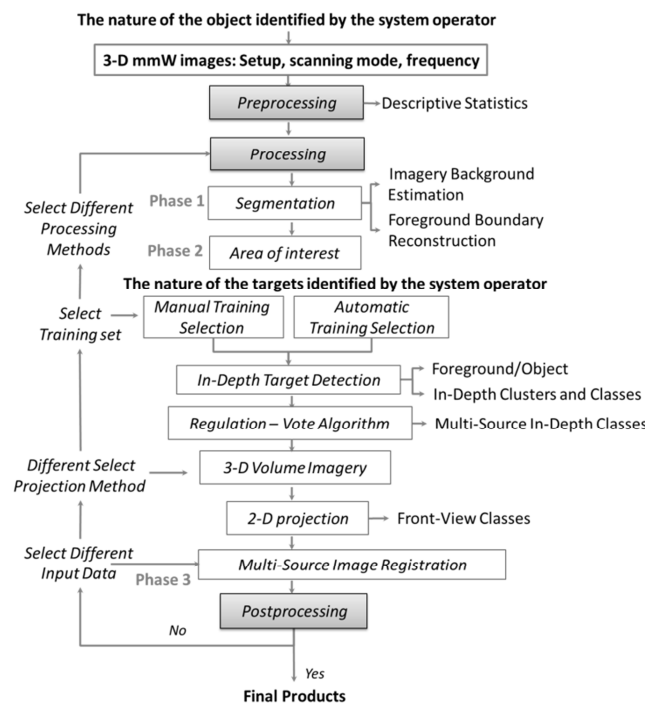


Figure 2. Flow-chart for image processing methodology

¹ The calibration sample is a sandwich-structured Rohacell sample between glass fiber layers with foreign inclusions on specific locations. The sample size is 399x199 mm and the total thickness is between 7 to 8mm. The defects are represented by several types of materials including Teflon, paper sheets, polyethylene, films and air and their sizes are vary between 6x6 mm, 12x12 mm and 25x25 mm.

3. Results

The obtained results illustrate the potential of image analysis to detect and extract defects and in-homogeneities (targets) within the manufactured calibration samples (objects). The structure of this section is representative to the hierarchical methodology, where each subsection presents and compares the obtained results for each stage of the analysis. Manual evaluation of detected targets is performed by calculating probabilities of detection (PD) and false alarms. PD was defined as the number of detected classes divided by the total number of manufactured defects. False alarms are defined as the number of false alarm classes. A quantitative assessment of the method's performance was provided by using the confusion matrices between number of pixels in each detected class and manual classification performed by an expert and considered as a ground truth.

3.1 Image Processing Phase 1 - Segmentation

The proposed algorithm [15-16] computes an independent constructive solution to the global background and non-intersecting noisy areas (stationary level) of the image. It is able to operate in parallel by multiple propagating contours that correspond to the boundaries of the expanding foreground, whereas the background is equal to zero. All image pixels are either zero or carry a value of significance of detection for the possible boundary. The results are the reconstructed 3-D foreground and object boundaries based on 2-D top and profiles views at 1-mm slice interval images.

3.2 Image Processing Phase 2 - Area of Interest Detection

The overall process is composed of segmentation and classification tasks executed on 2-D top and profiles views at 1-mm slice interval images. The proposed technique uses the information about the class membership and its relation to a certain cluster in order to classify new unknown candidates in one of the known classes. For that purpose, two assumptions have been made: a. the general description is a disk-shape cluster; b. the number of classes can be predefined. The first stage is performed by applying the k-Nearest Neighbors (kNN) algorithm, which segment all pixels included within the previously detected boundaries. The classification is adjusted by expectation-maximization (EM) algorithms (combining supervised maximum likelihood (ML-EM) and unsupervised K-Means and vote rule decision fusion techniques) to maximize the posterior probability of detection (Figure 4).

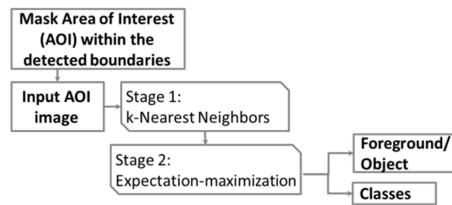


Figure 4. Image Processing Phase 2 – Flow chart for classification process.

Due to trade-offs regarding speed, accuracy and automation, the classification depends on the training set (known input data) and its selection (manual or automatic). In the proposed study the automatic training was executed by classifier iterations and is a part of an automatic learning technique. Whenever the manual selection is done, the system operator uses a dedicated program for visual detection and marks on the multilevel segmentation product.

The result of this process distinguishes between potential classes (related to the further target detection and recognition) within the object and its general area (foreground) based on 2-D top and profile views sliced images. The images are generated into 3-D volume imagery (Figure 5) using a Simultaneous Algebraic Reconstruction Technique (SART) [17].

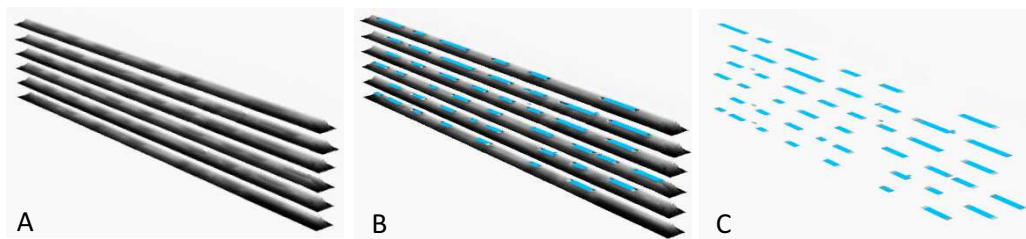


Figure 5. The generated 3-D results of the processed 2-D top-view (in-depth) image. A is the product of the segmentation stage, B is the detected classes on top of the segmentation, C is the detected classes.

3.3 Image Processing Phase 3 – Image Registration and Integration

The detected in-depth classes are gathered into join 3-D volume image following several combination rules. The vote rule decision fusion algorithm is a simplest technique applied on multiple classifiers assuming that output each classifier is a single class label [20]. This method applies general approximation, which expresses the strength (in relative weight system) of belief that the given object truly belongs to the particular cluster/class. In the boundary-based approach (kNN and ML-EM), vote values (relative weights) are computed in a straight-forward binary confidences calculation. In practice the output classes are expressed as decision vector $k = [k_1, \dots, k_n]^N$ (N is a total number of classes) where $k_i \in \{class_1, \dots, class_n, rejection\}$ and the general voting routine determined by binary characteristic function: 1 if $k_i = class_i$; 0 if $k_i \neq class_i$.

The obtained 3-D volume imagery are used to detect and extract the in-depth location of each class and forward project it (corresponding generation [18] or object-order rendering technique [19]) on the 2-D front-view image using the internal geometry and dimensions of the scanned object. Consecutively, the detected volumes of interest were marked as a rectangular label on the 2-D front-view images.

The feature-based automatic registration techniques were applied on the multi-source imagery data. These methods generally consist of four steps: 1. control points (CPs) extraction, 2. transformation model determination, 3. image transformation and re-sampling, and 4. registration accuracy assessment. The CPs were chosen by three algorithms: 1. automatic Harris corner detector, 2. SIFT-based sequence registration (Scale Invariant Feature Transform) and 3. Speeded-Up Robust Features (SURF) applied on the front-view images and re-sampled foreground boundaries. The results of SIFT and SURF are highly correlated and are equally different from the results of an automatic Harris corner detector. The possible explanation for that might be the dependency between the performance of the Harris corner detector and the image quality. Results shown in Table 1 confirm that both SIFT and SURF registration performances are more accurate than the Harris corner detector compared to the ground truth data.

Table 1. The registration results evaluated by the overall accuracy and Kappa coefficient²[21]. The illustrated results are in range of moderated agreement (0.4-0.6) and substantial agreement (0.61-0.8).

	Harris	SIFT	SURF
Overall Accuracy (%)	51	86	85
Kappa Coefficient (k)	0.42	0.7	0.68

Figure 6 shows the 2-D projected results of three classifiers (K-Means, ML-EM Euclidean distance, ML-EM Manhattan distance) applied on kNN segmented 300 GHz reflection image (phase 1) of the calibration sample accompanied by the ground truth and a digital photo of the sample. The classification products and the ground truth were registered applying the SIFT-based technique. The main differences between the detected classes are related to the nature of the classification methods. The unsupervised K-Means approach is more sensitive to the overall quality of the segmentation product, and thus the detected classes are less accurate (Table 2). The ML-EM is an iterative technique for optimizing the probability of detection. This classifier performed equally well for both automatic and manual training set selections. Results shown in Table 2 confirm that ML-EM performed slightly better by calculation of Euclidian distance rather than Manhattan distance.

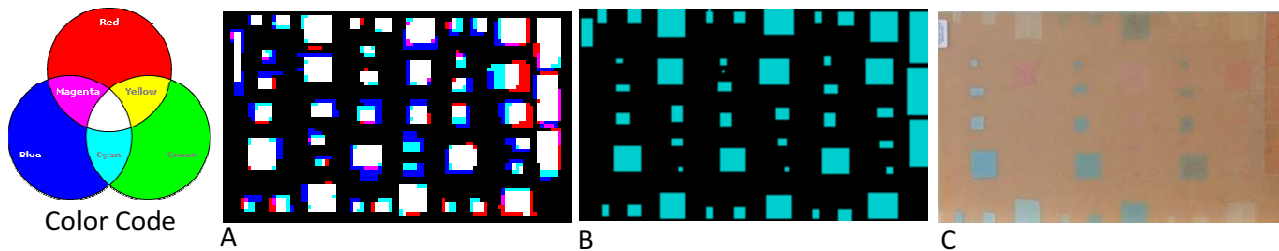


Figure 6. The 2-D classes of the 3-D volume of interest projected by object-order rendering technique. A is the product of classification stage – Red is the K-Means, Blue is the ML-EM Manhattan distance and Green is the ML-EM Euclidean distance; B is the ground truth; C is a digital photo of the calibration sample.

Table 2. The classification results evaluated by the overall accuracy and Kappa coefficient. The illustrated results are in range of substantial agreement (0.61-0.8).

	K-Means	ML-EM Manhattan	ML-EM Euclidean
Overall Accuracy (%)	73	84	86
Kappa Coefficient	0.54	0.69	0.7
PD (%)	95	100	100
False Alarm	2	2	1

4. Conclusions and Future Work

The proposed technique is able to detect internal (in-depth) defects within the 3-D multi-layer composite materials without any a priori knowledge of the targets. Using the multi-phase process that first extract foreground area of interest and then apply multi-stage semi-supervised classification technique, enables to detect the targets even in case of roughly segmented (poor quality) images. Detection of targets based on fully integrated information and target identification are important issues that must be addressed in a future work.

5. Acknowledgments

The authors would like to thank Fraunhofer-Institute, SynView GmbH for Physical Measurement techniques and Centro de Tecnologias Aeronauticas for their valuable contribution to this paper.

6. References

[1] J.B. Macqueen, “Some Methods for Classification and Analysis of Multivariate Observation,” in Proc 5th Berkeley Symposium on Mathematical Statistics and Probability, 281-297 (2002).

² Kappa coefficient is a quantitative estimation of the magnitude of agreement between classifiers measured between 0-less than chance agreement and 1- almost perfect agreement. $k=(Pr(a)-Pr(e))/(1-Pr(e))$ where $Pr(a)$ is the detected classes and $Pr(e)$ is the ground truth.

- [2] I.J. Myung, "Tutorial on maximum likelihood estimation," *Journal of Mathematical Psychology* 47, 90-100 (2003).
- [3] K.P. Murphy, "Naïve Bayes classifiers," Department of Computer Science, University of British Columbia.
- [4] C. am Weg, W. von Spiegel, B. Hils, T. Löffler, H. G. Roskos, "Fast active THz camera with range detection by frequency modulation," in *Proc IRMMW* 2008.
- [5] , R.J. Dengler, K.B. Cooper, G. Chattopadhyay, I. Mehdi, E. Schlecht, A. Skalare, C. Chen P.H. Siegel, "600 GHz imaging radar with 2 cm range resolution," 2007 IEEE MTT-S Intern. Microwave Symp. Digest, Honolulu, HI, 1371–1374 (2007).
- [6] M. Egmont-Petersena, D. de Ridderb, H. Handelsec, "Image processing with neural networks—a review," *Pattern Recognition* 35, 2279–2301(2002).
- [7] E. Cristofani, A. Brook, M. Vandewal, C. Matheis, J. Jonuscheit "Assessment of 3D signal and image processing using FMCW THz signals," In *Proc. of the OPTRO 2012, 5th International Symposium on Optronics in Defense and Security*, Paris, France, February 2012.
- [8] M. Vandewal, "Development and Optimization of THz NDT on aeronautics copposite multilayered structures," in *Proc SPIE* 8363 (1) 2012.
- [9] J. C. Dickinson, T. M. Goyette and J. Waldman: High Resolution Imaging using 325 GHz and 1.5 THz Transceivers, Submillimeter-Wave Technology Laboratory, University of Massachusetts Lowell 175 Cabot St. Lowell, MA 01854 (1990).
- [10] R. Appleby, "Passive millimetre-wave imaging and how it differs from terahertz imaging",*The Royal Society*, 10.1098/rsta.2003.1323, 379- 394 (2003).
- [11] E. N. Grossman, A. Luukanen, and A. J. Miller, "Terahertz active direct detection imagers," *Proc. SPIE*, 5411, 68–77 (2004)
- [12] R.W. McMillan, "Advances in Sensing with Security Applications". pp. 1 - 26, in J. Byrnes(ed.), *Terahertz Imaging Milimeter-Wave Radar*, Springer, Dordrecht, The Netherlands, 2006.
- [13] S. Kharkovsky and R. Zoughi, "Microwave and millimeter wave nondestructive testing and evaluation – Overview and Recent Advances," *IEEE Instrumentation and Measurement Magazine*, Vol.10(2), Apr. 2007, 26-38.
- [14] McLachlan, G., Peel, D., Whiten, W., "Maximum likelihood clustering via normal mixture model," *Signal Process. Image Commun.* 8, 105–111 (1996).
- [15] A. Brook, E. Cristofani, M. Vandewal, C. Matheis, J. Jonuscheit, "3-D Radar Image Processing Methodology for Defects Tracking of Aeronautics Composite Materials and Structures," in *Proc IEEE Radar conference*, Atlanta, USA, May 2012.
- [16] A. Brook, E. Cristofani, M. Vandewal, C. Matheis, J. Jonuscheit, R. Beigang, "A 3-D THz Image Processing Methodology for a Fully Integrated, Semi-Automatic and Near Real-Time Operational System,"in *Proc SPIE* 8363 (1) 2012.
- [17] A.H. Andersen, "Algebraic reconstruction in ct from limited view," *IEEE Tran. on Medical Imaging*, 8(1) 50-55 (1989).
- [18] M. Chen, L. Williams, "View Interpolation For Image Synthesis," in *Proc SIGGRAPH '93*, 279-288 (1993).
- [19] A. Kaufman, K. Mueller, "Overview of Volume Rendering," *Visualization Handbook*, eds. C. Johnson and C. Hansen, Academic Press (2005).
- [20] D. Ruta, B. Gabrys, "An overview of classifier fusion methods," *Computing and Information Systems* 7, 1-10 (2000).
- [21] J. Cohen, "A coefficient of agreement for nominal scales," *Educational and psychological measurement* 46, 20–37 (1960).